 DOI: 10.17344/acsi.2017.3192 *Acta Chim. Slov.* **2017,** *64,* 342–348

Scientific paper

$[M^{II}(NCS)_2(nia)_2(OH_2)_2]$: Preparation, Crystal Structure and Thermal Properties (M^{II} = Mn, Fe; nia = nicotinamide)

Marta Počkaj,* Nives Kitanovski, Boris Čeh and Romana Cerc-Korošec

Faculty of Chemistry and Chemical Technology, University of Ljubljana, Večna pot 113, SI-1000 Ljubljana, Slovenia.

** Corresponding author: E-mail: E-mail: marta.pockaj@fkkt.uni-lj.si.*

Received: 10-01-2017

Abstract

Two novel isostructural coordination compounds of manganese(II) (**1**) and iron(II) (**2**) with common formulae $[M^{II}(NCS)_2(nia)_2(OH_2)_2]$ have been prepared from water solution of appropriate metal salt, nicotinamide and KSCN. Their crystal structures were determined by means of X-ray diffraction on single crystals. The mononuclear title compounds crystallize in a triclinic *P*–1 space group with six monodentate octahedrally arranged ligands around the metal centre. The coordination molecules are self-assembled with an extended network of hydrogen bonds into a three-dimensional structure. Additionally, **1** and **2** were characterized with infrared spectroscopy, magnetic measurements and thermal analysis.

Keywords: crystal structure; coordination chemistry; thiocyanate; nicotinamide; manganese(II); iron(II).

1. Introduction

The biological importance of transition metal ions such as manganese and iron cannot be denied:[1,2] manganese(II) ions act as cofactors in a variety of enzymes with a spectra of functions while the main roles of iron-containing species are electrons and oxygen transfer. Nicotinamide and thiocyanate also play an important role in biochemical processes. For example, in metabolism of thiocyanate several short-lived intermediates with antibacterial activity are formed and thus, significantly lowered levels of thiocyanate in the human body are damaging to the human host defense system.[3,4] On the other hand, nicotinamide is an amide of nicotinic acid (niacin, vitamin B_3) and is a precursor to nicotinamide adenine dinucleotide phosphate (NADP), which is crucial for ATP synthesis, redox reactions and ADP-ribose transfer reactions.[5] In addition, manganese and iron coordination compounds have received significant attention also in the field of enzyme-mimicking compounds.[6–9] All aforementioned facts are driving force for research in coordination chemistry resembling biological systems.

Nicotinamide and its analogues (isonicotinamide, picolinamide) possess three potential coordinating sites: endocyclic nitrogen atom and amide nitrogen and oxygen atom. Usually, the coordination takes place *via* ring N atom in a monodentate manner, though bridging also *via* amide O atom may follow as well. Similarly, the thiocyanate anion is typically bound monodentately, mostly *via* its N-end, following by additional bridging *via* its remaining S-end; the monodentate coordination *via* its S-end is the least common.[10] Combining both ligands, a variety of extended frameworks interconnected by hydrogen and/or coordination bonds leading to interesting physical properties, e.g. magnetism or catalytic activity, can be formed.[11] The Cambridge Structural Database contains only four structures of coordination compounds exclusively with thiocyanate and nicotinamide ligands at the same time:[10] with zinc(II) ($[Zn(NCS)_2(nia)_2]$, refcode KITGAW),[12] copper(II) ($[Cu(\mu_2\text{-}SCN)(nia)_2]_n$, refcode UFAXII),[13] cadmium(II) ($[Cd(\mu_2\text{-}SCN)_2(nia)_2]_n{\cdot}nH_2O$, refcode QIFMAT)[14] and mercury(II) ($[Hg(\mu_2\text{-}SCN)(NCS)(nia)]_n$, refcode KITFUP).[12] Three additional crystal structures containing coordinated water are also known: with copper(II) ($[Cu(NCS)_2(nia)_2(OH_2)]$, refcode GISJAU)[15], cobalt(II) ($[Co(NCS)_2(nia)_2(OH_2)_2]$, refcode TCNICO)[16,17] and nickel(II) ($[Ni(NCS)_2(nia)_2(OH_2)_2]$, refcode CIVRAC),[18,19] the latter two being isostructural with the title complexes. In this paper, we report on preparation, crystal structure, spectroscopic, magnetic and thermal properties of two

mononuclear coordination complexes with common formulae $[M^{II}(NCS)_2(nia)_2(OH_2)_2]$ (M = Mn, Fe).

2. Experimental

2. 1. Reagents and Physical Measurements

All reagents and chemicals were purchased from commercial sources and used without further purification. CHN elemental analyses were performed with a Perkin-Elmer 2400 CHN Elemental Analyzer. The infrared spectra were measured on solid samples using a Perkin-Elmer Spectrum 100 series FT-IR spectrometer equipped with an ATR sampling accessory. Magnetic susceptibility of the substance was determined at room temperature by the Evans method using powdered samples and a Sherwood Scientific MSB-1 balance with $HgCo(NCS)_4$ as a calibrant. Diamagnetic corrections were estimated from Pascal's constants and the effective magnetic moments were calculated using the equation: $\mu_{eff} = 2.828(\chi MT)^{1/2}$. Simultaneous thermogravimetric/dynamic scanning calorimetry (TG/DSC) measurements were performed on a Mettler Toledo TGA/DSC1 instrument under dynamic flow of air or argon, respectively. The flow rate of the gas was 100 mL min^{-1}. Around 5 mg of the sample was put into 150 μL platinum crucible and heated in a temperature range from 25 to 800 °C with a heating rate of 10 C min^{-1}. Empty crucible served as a reference. Blank curve was subtracted. Evolved gases were detected using a Balzers ThermoStar mass spectrometer. Evolved gases were introduced into mass spectrometer via 75 cm long heated capillary.

2. 2. Synthesis

$[Mn(NCS)_2(nia)_2(OH_2)_2]$ (1). To the mixture of $MnCl_2 \cdot 4H_2O$ (792 mg, 4.0 mmol), KSCN (777 mg, 8.0 mmol) and nicotinamide (977 mg, 8.0 mmol), 5 mL of distilled water was added. The reaction mixture was heated under reflux at 60 °C until the clear solution was obtained. The reaction flask was sealed and stored in a refrigerator at ~ 8 °C. After several days, colourless crystals suitable for X-ray structural analysis were obtained. Yield: 433 mg (24%). Anal. Calcd. for $C_{14}H_{16}MnN_6O_4S_2$: C, 37.25%; H, 3.57%; N, 18.62%. Found: C, 37.50%; H, 3.31%; N, 18.43%. μ_{eff} = 6.06 BM. $\tilde{\nu}_{max}$: 3400–3000 (O–H, N–H), 2096 (CN from SCN), 1668 (C=O), 1386 (CN from nia) cm^{-1}.

$[Fe(NCS)_2(nia)_2(OH_2)_2]$ (2). To the mixture of $FeSO_4 \cdot 7H_2O$ (83.4 mg, 0.30 mmol), KSCN (116.6 mg, 1.20 mmol) and nicotinamide (73.3 mg, 0.60 mmol), 4 mL of distilled water was added. The reaction mixtures was stirred and slightly heated until all the solid reactants dissol-

Table 1. Crystal data, data collection and structure refinement.

Crystal data	**1**	**2**
Formula	$C_{14}H_{16}MnN_6O_4S_2$	$C_{14}H_{16}FeN_6O_4S_2$
M_r	451.39	452.30
Cell setting, space group	Triclinic, *P*–1	Triclinic, *P*–1
a (Å)	7.5470(5)	7.5299(6)
b (Å)	8.2535(5)	8.1847(7)
c (Å)	9.1503(7)	9.0367(5)
α (°)	73.196(6)	73.000(6)
β (°)	69.039(6)	69.536(6)
γ (°)	65.917(6)	66.518(8)
V (Å^3)	479.02(6)	470.92(7)
Z	1	1
D_x (Mg m^{-3})	1.565	1.595
μ (mm^{-1})	0.940	1.056
F(000)	231	232
Data collection		
T (K)	150(2)	150(2)
No. of measured, independent and observed reflections	4273, 2490, 2199	4111, 2432, 2055
R_{int}	0.0186	0.0221
Refinement		
Refinement method	full-matrix least-squares refinement on F^2	full-matrix least-squares refinement on F^2
R (on F_{obs}), *wR* (on F_{obs}), *S*	0.0290, 0.0674, 1.076	0.0330, 0.0699, 1.051
No. of contributing reflections	2490	2432
No. of parameters/restraints)	140/0	140/0
$\Delta\rho_{max}$, $\Delta\rho_{min}$ (eÅ^{-3})	0.435, –0.320	0.448,–0.310

ved. The Erlenmeyer flask was then cooled down in a refrigerator and after 15 minutes, the yellowish crystals suitable for X-ray structural analysis were obtained. Yield: 37 mg (27%). Anal. Calcd. for $C_{14}H_{16}FeN_6O_4S_2$: C, 37.17%; H, 3.56%; N, 18.58%. Found: C, 37.30%; H, 3.24%; N, 18.34%. μ_{eff} = 5.63 BM. $\bar{\nu}_{max}$: 3400–3000 (O–H), 2101 (CN from SCN), 1663 (C=O), 1385 (CN from nia) cm^{-1}.

2. 3. Crystallography

For X-ray structure determination single crystals of both compounds were surrounded by silicon grease, mounted on the tip of glass fibres and transferred to the goniometer head in the stream of liquid nitrogen. Data were collected on a SuperNova diffractometer equipped with Atlas detector using CrysAlis software and monochromated Mo Kα radiation (0.71073 Å) at 150 K.[20] The initial structural model containing coordination molecule was obtained *via* direct methods using the *SIR*97 structure solution program.[21] A full-matrix least-squares refinement on F^2 magnitudes with anisotropic displacement parameters for all non-hydrogen atoms using *SHELXL*2013 was employed.[22] All H atoms were initially located in difference Fourier maps and were further treated as riding on their parent atoms with C(aromatic)-H distance of 0.95 Å. The positions of water hydrogens as well as amide ones were obtained from a difference Fourier map and refined freely in iron complex while the N-H and O-H distances in manganese compound were restrained to 0.87(2) and 0.85(2) Å, respectively. Details on crystal data, data collection and structure refinement are given in Table 1. Figures depicting the structures were prepared with *ORTEP*3 and *Mercury*.[23,24]

3. Results and Discussion

Both title compounds have been prepared by dissolving appropriate metal salt, KSCN and nicotinamide in water. If necessary the starting mixtures were heated mildly and after the clear solutions were obtained they were kept in a refrigerator at ~8 °C until the crystals formed. The single crystals suitable for X-ray structural analysis were first tested by means of infrared spectroscopy. In IR spectra of both title compounds there is a broad band between 3400–3000 cm^{-1} representing O–H and N–H stretching involved in extended hydrogen bond network. Considering stretching frequencies of N–C bond in a thiocyanate ion which appears at 2096 cm^{-1} in **1** and 2101 cm^{-1} in **2**, the N-end coordination of thiocyanate anion is also confirmed. The characteristic vibrations of nicotinamide bonds are in agreement with the theoretical study of Bakiler and coworkers, showing the usual coordination mode of nicotinamide *via* its endocyclic nitrogen atom.[25]

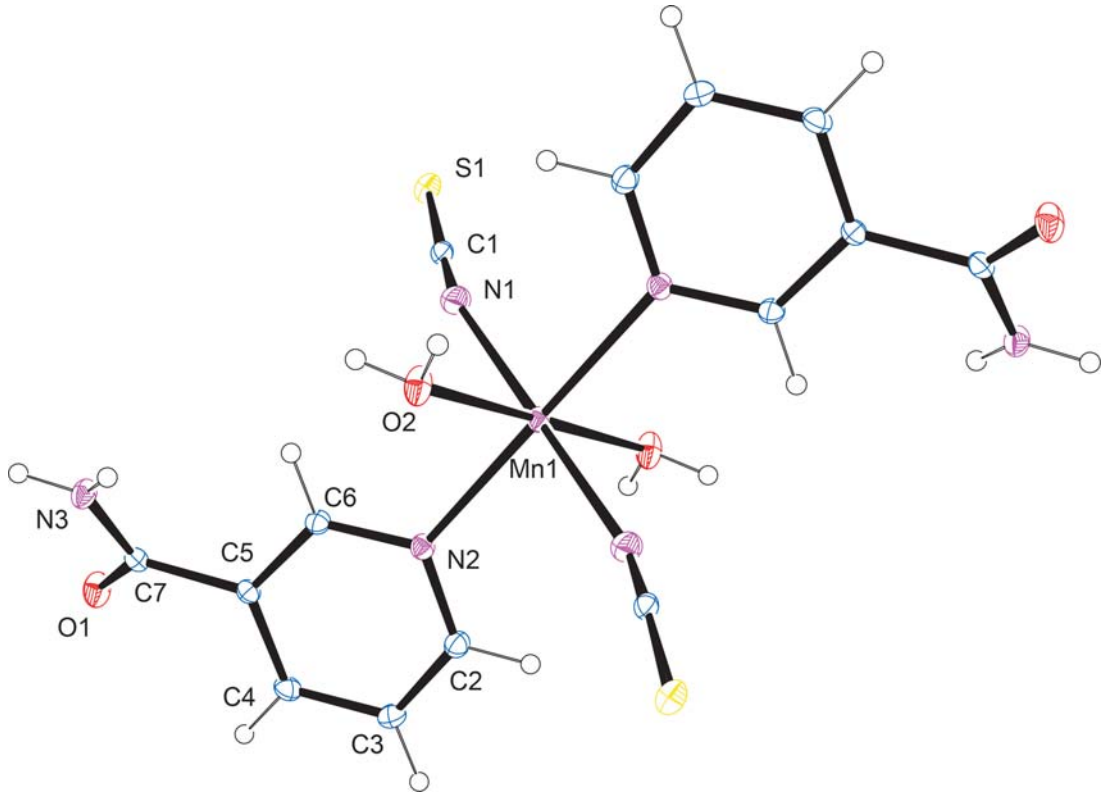

Figure 1. An ORTEP representation of coordination molecules in **1** with labels for atoms in asymmetric unit. Thermal ellipsoids are drawn at 30% probability level. Hydrogen atoms are represented as small spheres of arbitrary radii.

X-ray structural analysis has shown that both title coordination compounds are mononuclear (Fig. 1) with six-coordinated central metal ion in a shape of distorted octahedron. All three different ligands are bound in a monodentate mode: nicotinamide *via* endocyclic nitrogen and thiocyanate expectedly *via* its hard base *N*-end to both metals considered as hard acids according to Pearson principle.[26] The equatorial sites are occuppied by two oxygens from water (distance M–O1 2.1775(12) Å in **1** and 2.1015(14) Å in **2**) and by two nitrogens from NCS^- ligand (M–N1 distance of 2.1891(13) Å in **1** and 2.1398(17) Å in **2**). The bulkier and sterically more demanding nicotinamide ligand complements the first coordination sphere at axial positions (M–N2 distance of 2.2941(13) Å in **1** and 2.2225(14) Å in **2**). As observed, the bond distances in **2** are shorter than in **1** due to the smaller ionic radius of Fe^{2+} ion in comparison with Mn^{2+} (corresponding ionic radii for high-spin octahedral arrangements for Mn d^5 and Fe d^6 are 0.83 and 0.78 Å, respectively).[27] The pairs of equal ligands are *trans* to each other and due to symmetry restrictions (metal ion is located on an inversion centre) the angles *trans* ligand-M-*trans* ligand are constrained to 180°. The geometry of NCS^- ligand deviates only slightly from linearity, with the N–C–S angle of 178.11(14)° in **1** and 178.25(17)° in **2**, respectively. However, it is not bound in a completely linear fashion as the C–N–M angles are 156.42(13)° in **1** and 157.97(15)° in **2**, respectively. Several other bond distances and angles are collected in Table 2. The pyridine ring of nia ligand is almost planar with maximum deviation from the meanplane of – 0.011(2) Å for C4 (the values for **1** and **2** are the same) while the amide group is slightly out of pyridine-ring plane (torsion angles C6/C5/C7/N3 are 32.2(2)° in **1** and 31.9(3)° in **2**).

The coordination molecules are linked by extensive network of hydrogen bonds of O–H···O, O–H···S and N–H···S types forming a supramolecular structure (Fig. 2, Table 3). Hydrogen bonds donated by water oxygen link each coordination molecules with four adjacent and thus, layers stacking in *ac* plane/normal to (010) direction with thickness around ~8 Å are formed. Two additional N–H···S short contacts are present forming $R_4^2(8)$ rings as usual in related compounds:[28] the shorter stabilizes the aforementioned two-dimensional layers while the longer connects two neighboring layers into a three-dimensional structure. Thus, the sulphur atom of thiocyanate ligand is involved in a trifurcated hydrogen bonding motif. Weak π–π stacking is also observed between parallel pyridine rings of adjacent molecules with centroid-centroid distance of 3.8175(9) Å.

Table 2. Selected bond distances (Å) and angles (°) for complexes **1** and **2**.

	1	**2**
M–O2	2.1775(12)	2.1015(14)
M–N1	2.1891(13)	2.1398(17)
M–N2	2.2941(13)	2.2225(14)
N1–C1	1.159(2)	1.152(3)
C1–S1	1.6447(16)	1.651(2)
C7–O1	1.2353(18)	1.234(2)
C7–N3	1.329(2)	1.329(2)
O2–M–N1	90.65(5)	91.19(6)
O2–M–N2	91.17(5)	90.76(5)
N1–M–N2	87.05(5)	88.08(6)
N1–C1–S1	178.11(14)	178.25(17)
C1–N1–M	156.42(13)	157.97(15)

As already mentioned in the Introduction, several transition metal complexes with nia, SCN^- and in some cases also water have been structurally characterized till now.[12–19] Surprisingly, their preparation is simple and similar for all of them. On the other hand, their structures differ significantly: from mononuclear $[Zn(NCS)_2(nia)_2]$,[12] $([Cu(NCS)_2(nia)_2(OH_2)]$,[15] $([Co(NCS)_2(nia)_2(OH_2)_2]$,[16,17] $[Ni(NCS)_2(nia)_2(OH_2)_2]$[18,19] to polymeric $([Cu(\mu_2\text{-}SCN)(nia)_2]_n$,[13] $([Cd(\mu_2\text{-}SCN)_2(nia)_2]_n{\cdot}nH_2O$[14] and $[Hg(\mu_2\text{-}SCN)(NCS)(nia)]_n$.[12] In all cases, extensive hydrogen bonding is present. For mononuclear complexes the hydrogen

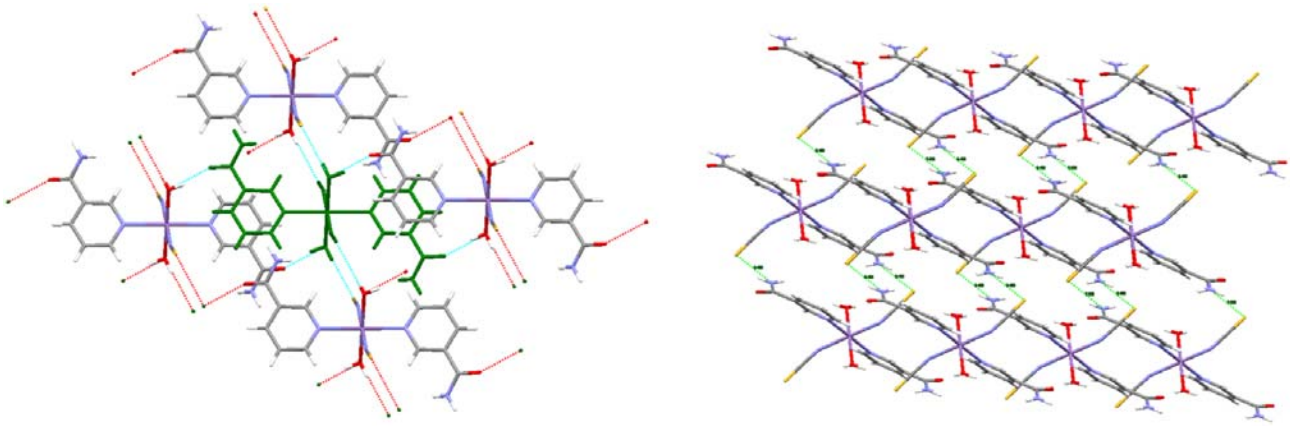

Figure 2. Hydrogen bond network/packing diagram in **1** leading to formation of layers (left) that get connected via N3–H3A···S1 hydrogen bond (right).

Table 3. Hydrogen bond geometry in **1** and **2**.

D–H···A	D–H (Å)	H···A (Å)	D···A (Å)	< D–H···A (°)
1				
O2–H2A···O1^{i}	0.84(3)	1.85(3)	2.6858(17)	170(2)
O2–H2B···S1^{ii}	0.81(3)	2.43(3)	3.2125(13)	163(2)
N3–H3B···S1^{ii}	0.83(2)	2.67(2)	3.4229(15)	151.0(18)
N3–H3A···S1^{iii}	0.88(2)	2.66(2)	3.4383(15)	147.9(16)
2				
O2–H2A···O1^{i}	0.816(15)	1.866(16)	2.6713(18)	169(2)
O2–H2B···S1^{ii}	0.825(16)	2.397(17)	3.2002(14)	164(2)
N3–H3B···S1^{ii}	0.848(15)	2.635(17)	3.4186(16)	154(2)
N3–H3A···S1^{iii}	0.872(15)	2.656(17)	3.4365(17)	149.6(18)

Symmetry codes: (*i*) *x*, *y*, *z* + 1; (*ii*) –*x*, –*y* + 1, –*z* + 1; (*iii*) *x*, *y* – 1, *z*.

bond scheme seems to be less uniform (N–H···O and N–H···S, usually not forming any ring motifs) but it always leads to 3D self-assembly of isolated coordination molecules. In polymeric complexes with four-coordinated metal, i.e. $[Hg(\mu_2\text{-SCN})(NCS)(nia)]_n$[12] and $([Cu(\mu_2\text{-SCN})(nia)_2]_n$,[13] chains are formed, while in polymeric complex $[Cd(\mu_2\text{-SCN})_2(nia)_2]_n \cdot nH_2O$[14] with six-coordinated Cd(II) layers are present. Chains or layers are further hydrogen bonded – in this case N–H···O hydrogen bonds are highly prevalent – resulting again in a formation of 3D structures.

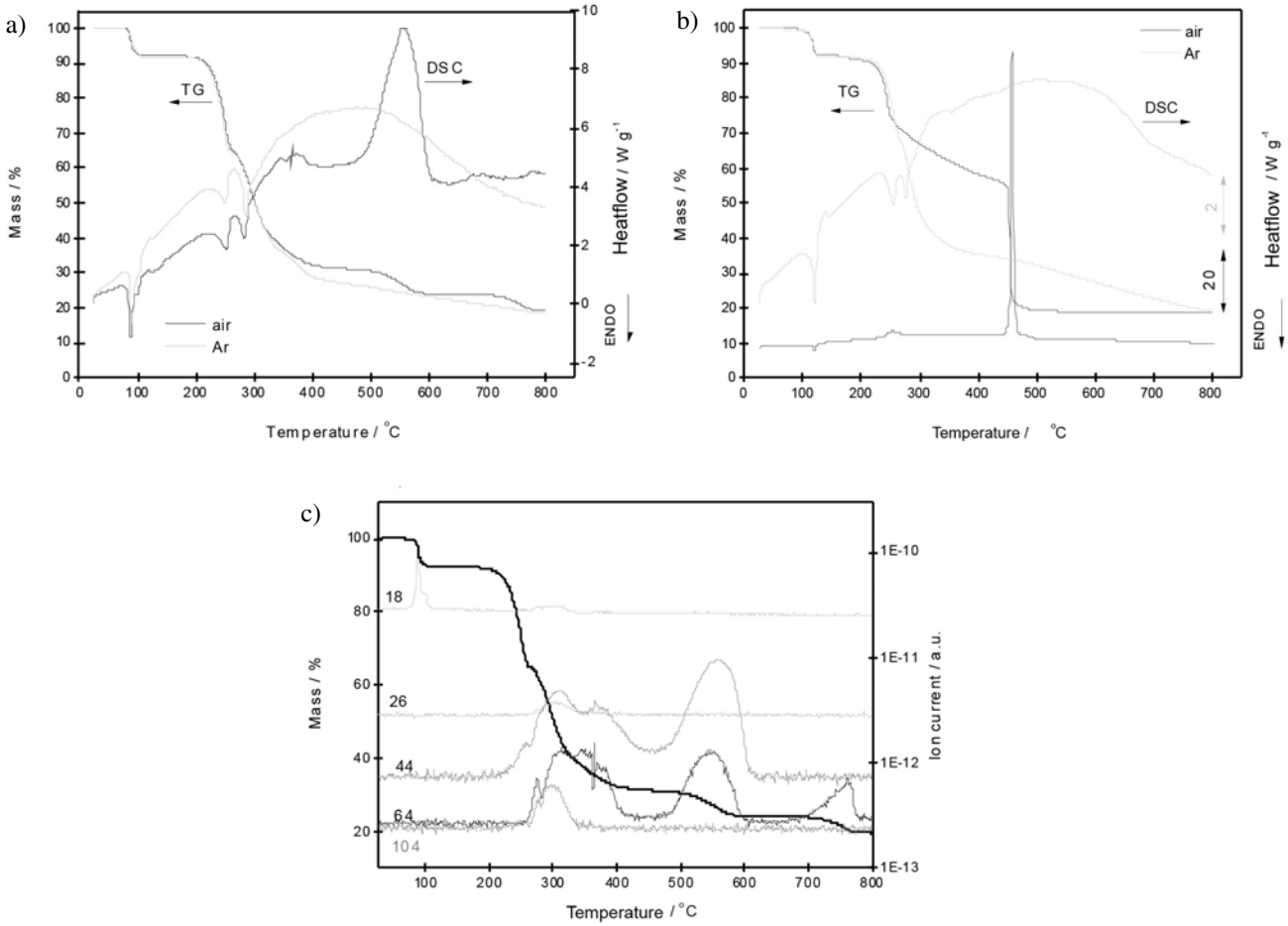

Figure 3. TG and DSC curves of a) Mn complex (**1**) and b) Fe-complex (**2**), and c) TG-MS curve of Mn complex (**1**) under air atmosphere. Note that in Fig. b two different scales on a DSC curve are presented, due to reducing the enthalpy signal under air atmosphere the first and the second DSC signals are not clearly seen.

In all cases D···A distances are comparable to those in the title compounds.

Thermal decomposition of both prepared complexes under air and argon atmosphere are shown in Figure 3. In the first step of thermal decomposition (70–110 °C for **1** and 85–130 °C for **2**) dehydration took place; evolution of water molecules is evident from a MS curve of Mn compound (see Figure 3c). Due to very similar molecular mass of both complexes, a theoretical mass loss for the dehydration process is the same for both complexes, 8.0 %, and that completely corresponds to the experimental value. At temperatures higher than 200 °C both complexes decompose further through several successive steps. Thermal decomposition of **1** is similar under air and argon atmosphere: from 200 to 270 °C sample lost 27 % and from 270 to 400 °C another 33.3 % under air and 37.5 % under argon atmosphere; overlapped reactions were endothermic. On MS curve evolution of CO_2 (m/z = 44) was observed at the beginning of the described decomposition reactions, followed by a multitude of other signals: water (m/z = 18), SO_2 (m/z = 64), CN^- (m/z = 26); also m/z = 104, the signal most close to molecular peak of nicotinamide (m/z = 122). The high number of observed signals (22 altogether) indicates the complexity of the thermal decomposition of the described complex. After 300 °C the route of thermal decomposition became different; under air atmosphere there are two distinct steps between 400 and 800 °C, the first being exothermic while under argon atmosphere there is a continuous mass loss up to 800 °C. The total mass loss under air atmosphere is 80.4 % meaning that Mn complex most probably decomposed to MnO_2 (theoretical mass loss 80.7 %) and 81.5 % under argon atmosphere. Theoretical mass loss for decomposition to Mn_2O_3 is 82.5 %, which most probably means that under argon atmosphere a final residue is a mixture of MnO_2 and Mn_2O_3.

The course of thermal decomposition of both Fe and Mn complex is very similar under argon atmosphere. The observed mass loss in a whole temperature range from 25 to 800 °C correspond to Fe_2O_3 (measured value 81.4%, theoretical 82.3%). Under air atmosphere thermal decomposition from 270 °C onward differ much with regard to thermal decomposition under argon; the rate of decomposition became slower, but at 450 °C a sharp exothermic step with a mass loss of around 35 % took place, leading to the same residue as obtained in argon atmosphere.

4. Conclusions

Two novel, isostructural compounds, namely $[Mn^{II}(NCS)_2(nia)_2(OH_2)_2]$ (**1**) and $[Fe^{II}(NCS)_2(nia)_2(OH_2)_2]$ (**2**) have been isolated. Their crystal structures reveal *trans* octahedral slightly elongated $MN_2O_2N_2$ chromophores. Despite shorter M–O coordination bonds the water molecules are removed first at an elevated temperature, as expected. All three ligands enable H-bonds, thus building a 3D structure of mononuclear building blocks. Due to a lack of any coordination bridging weak magnetic interactions within solids among the metal centers are expected. On the other hand, strong intermolecular ability via H-bonding, especially in water, for the title manganese(II) and iron(II) compounds is noticed. Thermal decomposition of both complexes is similar losing water in first step of mass loss while in the remaining steps other ligands decompose yielding Fe_2O_3 or a mixture of MnO_2 and Mn_2O_3, respectively.

5. Supplementary Information

CCDC 1498589 (**1**) and 1498590 (**2**) contain the supplementary crystallographic data. These data can be obtained free of charge from The Cambridge Crystallographic Data Centre via www.ccdc.cam.ac.uk/data_request/cif.

6. Acknowledgments

The authors thank Mateja Kožar and Silva Peternel for their assistance during synthesis. This work was financially supported by Slovenian research agency (grant P1-0175). The EN-FIST Centre of Excellence is also acknowledged for the use of SuperNova diffractometer.

7. References

1. C. A. Dlouhy, C. E. Outten, in: L. Banci (Ed.): Metallomics and the Cell. Springer Science+Business Media, Dordrecht, The Netherlands, **2013**, pp. 241–278. https://doi.org/10.1007/978-94-007-5561-1_8
2. A. N. Jensen, L. T. Jensen, in: L. G. Costa, M. Aschner (Ed.): Manganese in Health and Disease, Royal Society of Chemistry, Cambridge, UK, **2015**, pp. 1–33.
3. K. M. Pruitt, J. Tenovuo, R. W. Andrews, T. McKane, *Biochemistry* **1982**, *21*, 562–567. https://doi.org/10.1021/bi00532a023
4. G. E. Conner, C. Wijkstrom-Frei, S. H. Randell, V. E. Fernandez, M. Salathe, *FEBS Lett.* **2007**, *581*, 271–278. https://doi.org/10.1016/j.febslet.2006.12.025
5. D. MacKay, J. Hathcock, E. Guarneri, *Nutr. Rev.* **2012**, *70*, 357–366. https://doi.org/10.1111/j.1753-4887.2012.00479.x
6. M. Počkaj, B. Kozlevčar, N. Kitanovski, *Acta Chim. Slov.* **2015**, *62*, 272–280. https://doi.org/10.17344/acsi.2014.1048
7. *Concepts and models in bioinorganic chemistry,* 3. ed., Eds., H.-B. Kraatz, N. Metzler-Nolte, Wiley-VCH, Weinheim, **2006**.
8. C. Pettinari, R. Pettinari, *Coord. Chem. Rev.* **2005**, *249*, 663–691. https://doi.org/10.1016/j.ccr.2004.08.017

9. N. Kitanovski, N. Borsan, M. Kasunič, V. Francetič, J. Popović, I. Djerdj, X. Rocquefelte, J. Reedijk, B. Kozlevčar, *Polyhedron* **2014**, *70*, 119–124. https://doi.org/10.1016/j.poly.2013.12.029
10. F. H. Allen, *Acta Crystallogr. B* **2002**, *58*, 380–388. https://doi.org/10.1107/S0108768102003890
11. C. B. Aakeröy, J. Desper, J. Valdés-Martínez, *CrystEngComm* **2004**, *6*, 413–418. https://doi.org/10.1039/B410129B
12. M. Đaković, Z. Popović, G. Giester, M. Rajić-Linarić, *Polyhedron* **2008**, *27*, 465–472. https://doi.org/10.1016/j.poly.2007.09.036
13. C. Näther, I. Jeß, *Acta Crystallogr. C* **2002**, *58*, m190–m192. https://doi.org/10.1107/S0108270102001592
14. G. Yang, H.-G. Zhu, B.-H. Liang, X.-M. Chen, *J. Chem. Soc., Dalton Trans*. **2001**, 580–585. https://doi.org/10.1039/b009129o
15. C. Li, W. Ding, C. Shao, *Acta Crystallogr. E* **2008**, *64*, m314–m314. https://doi.org/10.1107/S1600536807068511
16. R. E. Marsh, *Acta Crystallogr. B* **2005**, *61*, 359–359. https://doi.org/10.1107/S0108768105009651
17. D. Pandey, S. S. Narvi, S. Chaudhuri, *Acta Crystallogr. E* **2014**, *70*, m236–m236. https://doi.org/10.1107/S1600536814011453
18. D. Pandey, S. S. Narvi, G. K. Mehrotra, R. J. Butcher, *Acta Crystallogr. E* **2014**, *70*, m183–m183. https://doi.org/10.1107/S1600536814006771
19. D. Pandey, S. S. Narvi, G. K. Mehrotra, R. J. Butcher, *Chin. J. Struct. Chem*. **2015**, *34*, 777–785.
20. CrysAlis PRO, Oxford Diffraction Ltd, Yarnton, Oxfordshire, England, **2011**.
21. A. Altomare, M. C. Burla, M. Camalli, G. L. Cascarano, C. Giacovazzo, A. Guagliardi, A. G. G. Moliterni, G. Polidori, R. Spagna, *J. Appl. Cryst.* **1999**, *32*, 115–119. https://doi.org/10.1107/S0021889898007717
22. G. M. Sheldrick, *SHELXL*2013, University of Göttingen, Germany, **2013**.
23. L. J. Farrugia, *J. Appl. Crystallogr*. **1997**, *30*, 565–565. https://doi.org/10.1107/S0021889897003117
24. C. F. Macrae, P. R. Edgington, P. McCabe, E. Pidcock, G. P. Shields, R. Taylor, M. Towler, J. van de Streek, *J. Appl. Cryst*. **2006**, *39*, 453–457. https://doi.org/10.1107/S002188980600731X
25. M. Bakiler, O. Bolukbasi, A. Yilmaz, *J. Mol. Struct*. **2007**, 826, 6–16. https://doi.org/10.1016/j.molstruc.2006.04.021
26. R. G. Pearson, *J. Am. Chem. Soc.* **1963**, *85*, 3533–3539. https://doi.org/10.1021/ja00905a001
27. R. D. Shannon, *Acta Crystallogr. A* **1976**, *32*, 751–767. https://doi.org/10.1107/S0567739476001551
28. M. Đaković, J. Jaźwiński, Z. Popović, *Acta Chim. Slov*. **2015**, *62*, 328–336. https://doi.org/10.17344/acsi.2014.1128

Povzetek

Iz vodne raztopine, ki je vsebovala nikotinamid, KSCN in ustrezno sol kovine(II), smo pripravili dve novi, izostrukturni, koordinacijski spojini mangana(II), **1**, in železa(II), **2**, s splošno formulo $[M^{II}(NCS)_2(nia)_2(OH_2)_2]$. Na osnovi difrakcije na monokristalu smo določili kristalni strukturi obeh spojin, ki kristalizirata v triklinski prostorski skupini *P*–1. Spojini sta enojedrni, centralni atom pa je v obeh koordiniran oktaedrično s šestimi ligandi. Koordinacijske molekule so povezane v tridimenzionalno strukturo s pomočjo vodikovih vezi. Spojini **1** in **2** smo okarakterizirali tudi z infrardečo spektroskopijo, magnetnimi meritvami in termično analizo.